Substrate Integrated Waveguide Filter With Flat Passband Based on Complex Couplings

Liang-Feng Qiu, *Member, IEEE*, Lin-Sheng Wu, *Senior Member, IEEE*, Bing Xie, Wen-Yan Yin, *Fellow, IEEE*, and Jun-Fa Mao, *Fellow, IEEE*

***Abstract*— A lossy filter with flat passband and asymmetric response is proposed by using complex couplings. The complex coupling coefficients with positive and negative imaginary parts are realized with transmission lines loaded with series and shunt resistors, respectively. Design formulas are derived for the critical parameters. A filter prototype is developed at 4.97 GHz and substrate integrated waveguide resonators with unloaded Q-factor of 450 are used. One transmission zero is located in its upper stopband. The 0.2-dB bandwidth of 279 MHz is achieved and the equivalent Q-factor is about 1900. Good agreement is obtained among the synthesized, simulated, and measured results.**

***Index Terms*— Complex coupling, lossy bandpass filter, substrate integrated waveguide (SIW), uniform Q-factor.**

I. Introduction

THE design of high-performance miniaturized bandpass filters is always a challenge, due to relatively low unloaded Q-factors of compact resonators. Low-Q filters suffer from degraded inband insertion loss (IL), passband flatness, and frequency selectivity, especially for narrowband applications.

In some applications, small inband magnitude variation, i.e., flat passband, is highly required while the additional IL can be tolerated, such as in a satellite input multiplexer and alternative receiver architectures [1]. In order to achieve flat passband and good selectivity with low-Q structures, the synthesis methods of bandpass filters with the consideration of loss have drawn much attention. Some techniques are proposed. The predistortion technique achieves good passband flatness by reflecting more power in the middle passband [2], resulting significantly deteriorated return loss (RL). The nonuniform-Q filters have improved the inband performance by controlling the Q-factor ratio of the resonators [3], with the degradation of RL and transmission zeros. The lossy coupling filters have the same performances as the ideal ones except for the additional attenuation [4], [5], which may be compensated by preamplifiers. Thus, the lossy coupling method is one attractive candidate for the high-performance miniaturized filter design. For a symmetric response, the lossy filter can be designed only with purely reactive and resistive couplings [6], [7]. As synthesized in [5], complex couplings with both nonzero real and imaginary parts will be required when an asymmetric response with transmission zero(s) is desired. Thus, the complex coupling is to be realized as the key issue to build up this kind of lossy filter.

Manuscript received November 22, 2017; revised February 12, 2018; accepted April 15, 2018. Date of publication May 9, 2018; date of current version June 5, 2018. This work was supported by the National Science Foundations of China under Grant 61370008 and Grant 61327803. *(Corresponding author: Lin-Sheng Wu.)*

The authors are with the Key Laboratory of Ministry of Education of Design and Electromagnetic Compatibility of High-Speed Electronic Systems, Shanghai Jiao Tong University, Shanghai 200240, China (e-mail: wallish@sjtu.edu.cn).

Color versions of one or more of the figures in this paper are available online at http://ieeexplore.ieee.org.

Digital Object Identifier 10.1109/LMWC.2018.2829349

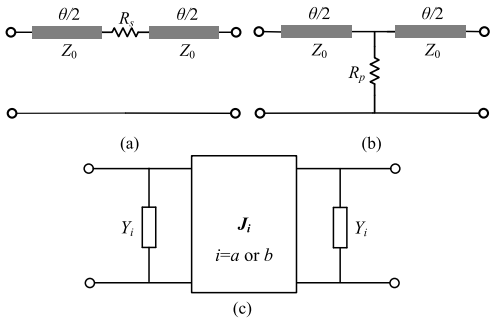

Fig. 1. Proposed transmission lines loaded with (a) series and (b) shunt resistors, and (c) equivalent model.

In this paper, a substrate integrated waveguide (SIW) lossy filter is proposed to achieve an asymmetric response. Different from the Chebyshev SIW filter in [6] and [7], complex coupling coefficients should be applied in this paper, which are realized with transmission lines loaded with series and shunt resistors. The complex-coupled filter with one transmission zero is built up by uniform-Q resonators. Good performance is achieved.

II. Analysis and Design

Fig. 1(a) and (b) shows the two-port circuit models for the complex couplings whose imaginary parts are positive and negative, respectively. Both circuits can be equivalent to a J-inverter with a complex immittance and two residual shunt complex admittances at two ports, as shown in Fig. 1(c).

The ABCD matrixes $\mathbf{A}_a$ of the circuit in Fig. 1(a) and $\mathbf{A}_c$ of its equivalent circuit in Fig. 1(c) are calculated by

$$\mathbf{A}_a = \begin{bmatrix} \cos\theta + j\dfrac{R_s \sin\theta}{2Z_0} & \dfrac{1+\cos\theta}{2}R_s + jZ_0\sin\theta \\ \dfrac{\cos\theta - 1}{2Z_0^2}R_s + j\dfrac{\sin\theta}{Z_0} & \cos\theta + j\dfrac{R_s\sin\theta}{2Z_0} \end{bmatrix} \quad (1)$$

$$\mathbf{A}_c = \begin{bmatrix} jY_a/J_a & j/J_a \\ j\left(Y_a^2/J_a + J_a\right) & jY_a/J_a \end{bmatrix}. \quad (2)$$

By making (1) and (2) equal to each other, the equivalent admittance J_a of the J-inverter and the residual admittance Y_a of the shunt circuit shown in Fig. 1(c) for Fig. 1(a) are obtained by

$$J_a = \frac{4Z_0\sin\theta}{D_a} + j\frac{2R_s(1+\cos\theta)}{D_a} \quad (3)$$

$$Y_a = \frac{2R_s(1+\cos\theta)}{D_a} + j\frac{R_s^2\sin\theta(1+\cos\theta) - 2Z_0^2\sin 2\theta}{Z_0 D_a} \quad (4)$$

where

$$D_a = R_s^2(1+\cos\theta)^2 + 4Z_0^2\sin^2\theta. \quad (5)$$

Similarly, the equivalent admittance J_b of the J-inverter in Fig. 1(b) and the residual admittance Y_b of the shunt circuit shown in Fig. 1(c) for Fig. 1(b) are deduced by

$$J_b = \frac{4R_p^2 \sin\theta}{Z_0 D_b} - \mathrm{j}\frac{2R_p(1-\cos\theta)}{D_b} \tag{6}$$

$$Y_b = \frac{2R_p(1-\cos\theta)}{D_b} - j\frac{Z_0^2 \sin\theta(1-\cos\theta)+2R_p^2 \sin 2\theta}{Z_0 D_b} \tag{7}$$

$$D_b = Z_0^2(1-\cos\theta)^2 + 4R_p^2 \sin^2\theta. \tag{8}$$

It is seen from (3) and (6) that the imaginary parts of inverter admittances for the circuits of Fig. 1(a) and (b) are positive and negative, respectively. Therefore, a flat-passband lossy filter with an asymmetric response can be realized by the circuits shown in Fig. 1(a) and (b) for the complex coupling coefficients.

The residual susceptance slope parameters b_a and b_b of the circuits shown in Fig. 1(a) and (b) can be derived by calculating the derivatives of $\mathrm{Im}(Y_a)$ in (4) and $\mathrm{Im}(Y_b)$ in (7) as

$$b_a = \frac{2Z_0^4 \sin^2\theta + R_s^4 \cos^6\frac{\theta}{2} - 2R_s^2 Z_0^2 \cos\theta \cos^4\frac{\theta}{2}}{4Z_0\left(R_s^2 \cos^4\frac{\theta}{2} + Z_0^2 \sin^2\theta\right)^2/\theta} \tag{9}$$

$$b_b = \frac{2R_p^4 \sin^2\theta + Z_0^4 \sin^6\frac{\theta}{2} + 2R_p^2 Z_0^2 \cos\theta \sin^4\frac{\theta}{2}}{4Z_0\left(Z_0^2 \sin^4\frac{\theta}{2} + R_p^2 \sin^2\theta\right)^2/\theta}. \tag{10}$$

The residual conductance and susceptance can be absorbed by the two adjacent resonators connected to the J-inverter. Thus, the resonant frequencies and susceptance slope parameters of the two resonators should be adjusted, accordingly, during the filter design. The resonant frequency f_r and the susceptance slope parameter b_{in} of the resonator are modified by

$$f_r \Leftarrow f_r[1 + 0.5\mathrm{Im}(Y_i)/b_{\mathrm{in}}] \tag{11}$$

$$b_{\mathrm{in}} \Leftarrow b_{\mathrm{in}} - b_i \tag{12}$$

where the subscript i represents a or b.

III. Design Equations

A third-order generalized Chebyshev lossy filter with a flat passband is designed as an example, which is centered at $f_0 = 5$ GHz with one transmission zero located at 5.39 GHz. The fractional bandwidth is FBW = 5% and the inband RL is 20 dB, and all the resonators share the same unloaded Q-factor of 450. The coupling matrix $\mathbf{M}$ of the filter is synthesized as [5], where NS and NL denote the nonresonating nodes connected to source and load nodes, respectively, and the normalized coupling coefficient between the nodes j and k is denoted by M_{jk}. The scaling factor, i.e. the coupling coefficient between the source and NS nodes (the load and NL nodes) [4], is $M_{S,\mathrm{NS}} = M_{\mathrm{NL},L} = 0.1898$. The coupled resonator circuit model and its coupling scheme of the developed filter are shown in Fig. 2.

The complex coupling M_{13} between the resonators 1 and 3 is realized with the structure shown in Fig. 1(a) while M_{12} and M_{23} are realized with the structure shown in Fig. 1(b), since the imaginary parts of M_{13} and M_{12} (M_{23}) are positive and negative, respectively. The inverter admittances J_{13} and J_{12} (J_{23}) are given as

$$J_{13} = M_{13}\mathrm{FBW}\sqrt{b_1^{(3)} b_3^{(1)}} \tag{13}$$

$$J_{12} = M_{12}\mathrm{FBW}\sqrt{b_1^{(2)} b_2^{(1)}} = J_{23} = M_{23}\mathrm{FBW}\sqrt{b_2^{(3)} b_3^{(2)}} \tag{14}$$

where $b_j^{(k)}$ is the susceptance slope parameter b_{in} of the node j seen from the node k. By comparing (3) with (13), the loaded resistance R_{13} and the characteristic impedance Z_{13} of the microstrip line between the resonators 1 and 3 are obtained by

$$R_{13} = 2\mathrm{Im}(M_{13})/\left[\mathrm{FBW}\sqrt{b_1^{(3)} b_3^{(1)}}|M_{13}|^2(1+\cos\theta_{13})\right] \tag{15}$$

$$Z_{13} = \mathrm{Re}(M_{13})/\left(\mathrm{FBW}\sqrt{b_1^{(3)} b_3^{(1)}}|M_{13}|^2 \sin\theta_{13}\right) \tag{16}$$

where θ_{jk} is the electrical length of microstrip line between nodes j and k. Similarly, R_{12} (R_{23}) and Z_{12} (Z_{23}) are derived by

$$R_{12} = R_{23} = \frac{(1-\cos\theta_{12})\mathrm{Re}^2(M_{12})}{-2\mathrm{FBW}\sqrt{b_1^{(2)} b_2^{(1)}}|M_{12}|^2 \sin^2\theta_{12}\mathrm{Im}(M_{12})} \tag{17}$$

$$Z_{12} = Z_{23} = \mathrm{Re}(M_{12})/\left(\mathrm{FBW}\sqrt{b_1^{(2)} b_2^{(1)}}|M_{12}|^2 \sin\theta_{12}\right). \tag{18}$$

The characteristic impedance of the 90° lines between the source (load) and the nonresonating nodes is obtained by

$$Z_{S,\mathrm{NS}} = Z_{\mathrm{NL},L} = 1/J_{S,\mathrm{NS}} = \sqrt{Z_p}/\left(M_{S,\mathrm{NS}}\sqrt{b_2^{(\mathrm{NS})}\mathrm{FBW}}\right) \tag{19}$$

where Z_p is the reference impedance of the I/O ports. When $Z_{S,\mathrm{NS}} = Z_{\mathrm{NL},L} = Z_p$, the two line sections can be absorbed by ports and the reference planes of source and load are shifted to the locations of the NS and NL nodes, respectively. The characteristic impedance of the microstrip line between resonator 1 (3) and the nonresonating node NS (NL) is

$$Z_{\mathrm{NS},1} = Z_{3,\mathrm{NL}} = 1/J_{\mathrm{NS},1} = 1/\left(M_{\mathrm{NS},1}\mathrm{FBW}\sqrt{b_1^{(\mathrm{NS})} b_2^{(\mathrm{NS})}}\right). \tag{20}$$

The resistance between resonator 2 and the nonresonating node NS (NL) is calculated by

$$R_{\mathrm{NS},2} = R_{2,\mathrm{NL}} = 1/\left[b_2^{(\mathrm{NS})}\mathrm{FBWIm}(-M_{\mathrm{NS},2})\right]. \tag{21}$$

The electrical length of the two sections of microstrip lines connected to the resistors $R_{\mathrm{NS},2}$ and $R_{2,\mathrm{NL}}$ are 180° and 360°.

IV. Results and Discussion

Here, we choose $b_1^{(3)} = b_3^{(1)} = b_1^{(2)} = b_2^{(1)} = b_2^{(3)} = b_3^{(2)} =$ 0.35 S, and $\theta_{12} = \theta_{23} = \theta_{13} = 90°$ for simplification. The values of $R_{13} = 39\ \Omega$, $Z_{13} = 154\ \Omega$, $R_{12} = R_{23} = 1500\ \Omega$, and $Z_{12} = Z_{23} = 58\ \Omega$ are obtained from (15)–(18). Set $b_2^{(NS)} = b_2^{(NL)} = 11.1$ S, then we have $R_{\mathrm{NS},2} = R_{2,\mathrm{NL}} = 383\ \Omega$

	NS	1	2	3	NL
NS	$-0.0047j$	0.2037	$-0.0047j$	0	0
1	0.2037	$0.0918-0.1087j$	$0.9818-0.0188j$	$0.3642+0.0457j$	0
2	$-0.0047j$	$0.9818-0.0188j$	$-0.3532-0.0913j$	$0.9818-0.0188j$	$-0.0047j$
3	0	$0.3642+0.0457j$	$0.9818-0.0188j$	$0.0918-0.1087j$	0.2037
NL	0	0	0	0.2037	$-0.0047j$

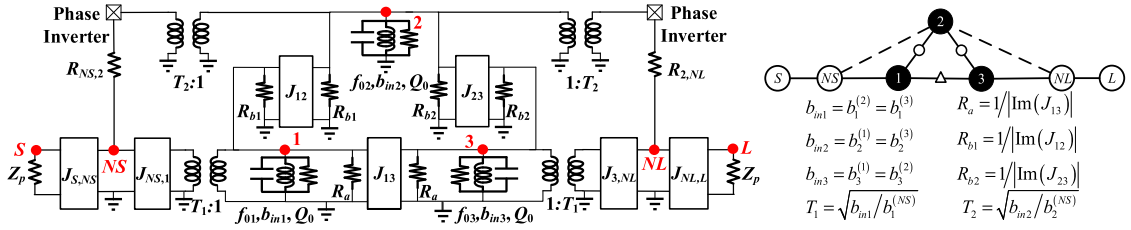

Fig. 2. Coupled resonator circuit model of the developed filter, where the coupling between the nonresonating node NS (NL) and resonator 2 is purely resistive, the coupling between resonators 1 and 2 (2 and 3) is with a complex coefficient whose imaginary part is negative, related to Fig. 1(b), and the coupling between resonators 1 and 3 is with a complex coefficient whose imaginary part is positive, related to Fig. 1(a).

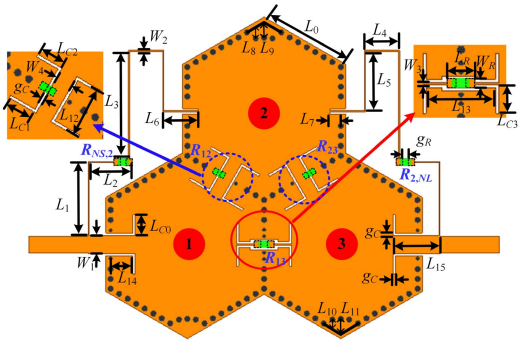

Fig. 3. Layout of the fabricated lossy filter with complex couplings. Geometrical parameters are $L_0 = 16.24$, $L_1 = 13.64$, $L_2 = 7.9$, $L_3 = 19.64$, $L_4 = 6.48$, $L_5 = 10.87$, $L_6 = 6.5$, $L_7 = 2$, $L_8 = 2$, $L_9 = 2.8$, $L_{10} = 1.6$, $L_{11} = 2.6$, $L_{12} = 7.34$, $L_{13} = 10.12$, $L_{14} = 4.1$, $L_{15} = 8.62$, $L_{C0} = 3.76$, $L_{C1} = 4.4$, $L_{C2} = 3.9$, $L_{C3} = 3.86$, $L_R = 3.6$, $W_R = 1.2$, $W_1 = 3.38$, $W_2 = 0.2$, $W_3 = 0.22$, $W_4 = 2.45$, $g_C = 0.4$, and $g_R = 1.2$ (unit: mm). The resistors (package size of 0603) are with $R_{\mathrm{NS},2} = R_{2,\mathrm{NL}} = 390\ \Omega$, $R_{12} = R_{23} = 1500\ \Omega$, and $R_{13} = 39\ \Omega$. The structure within the red solid circle is related to Fig. 1(a) while the structures within the blue dotted circles are related to Fig. 1(b).

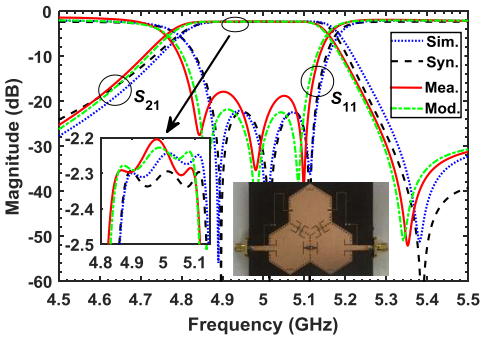

Fig. 4. Synthesized (Syn.), simulated (Sim.), measured (Mea.), and modified simulated (Mod.) results of the filter prototype.

from (21) and $Z_{S,\mathrm{NS}} = Z_{\mathrm{NL},L} = 50\ \Omega$ from (19) to remove these two line sections. Let $b_1^{(NS)} = b_3^{(NL)} = 0.4$ S, then $Z_{\mathrm{NS},1} = Z_{3,\mathrm{NL}} = 47\ \Omega$ is obtained from (20). According to (12), the susceptance slope parameters are slightly modified as $b_1^{(3)} = b_3^{(1)} = 0.345$ S, $b_1^{(2)} = b_2^{(1)} = b_2^{(3)} = b_3^{(2)} = 0.336$ S. The resonant frequencies of resonators 1–3 are 4.989, 5.044, and 4.989 GHz, respectively, according to (11). As shown in Fig. 3, the prototype is fabricated on a 40-mil-thick taconic TLY-5A substrate, with $\varepsilon_r = 2.17$ and $\tan\delta = 0.0009$, where the unloaded Q-factor of the hexagonal SIW resonators is about 450, extracted from the full-wave electromagnetic simulation. The physical dimensions and resistances of the filter are shown in Fig. 3. The 0603 resistors R_{12}, R_{23}, and R_{13} are mounted over slots on the top metal plane and the resistor R_{12} (R_{23}) is grounded by the metallic vias between SIW cavities. Note that the 390-Ω resistors, which are available in practice, are used instead of the 383-Ω resistors.

The synthesized, simulated, and measured S-parameters of the prototype are plotted in Fig. 4. Good agreement is achieved among them. The measured response is centered at 4.97 GHz with one transmission zero located at 5.35 GHz. The measured frequency shift of 30 MHz from the synthesized and simulated ones is mainly due to the tolerance of permittivity. By changing the permittivity to $\varepsilon_r = 2.2$ in simulation, the modified simulated response is also plotted in Fig. 4, which agrees well with the measured one. The difference of RLs between the measured and simulated results is mainly due to the fabrication tolerance. The measured minimum inband IL is 2.2 dB, which is almost the same as the synthesized and simulated values. The 0.2-dB bandwidth is about 279 MHz in measurement, which matches the synthesized and simulated ones well. This 0.2-dB bandwidth is equivalent to a lossless synthesized filter but realized with the uniform unloaded Q-factor of 1900. Compared with the lossless synthesized filter but realized with the uniform unloaded Q-factor of 450, the 0.2-dB bandwidth of the proposed lossy filter is broadened by 20%.

V. Conclusion

A lossy SIW filter with an asymmetric response and complex couplings is developed to improve passband flatness with uniform-Q resonators. The method is established with detailed design equations to realize complex coupling coefficients with positive and negative imaginary parts based on resistor-loaded transmission lines. An equivalent circuit model of the lossy filter is proposed and all the critical parameters can be obtained analytically. Good agreement is obtained among the synthesized, simulated, and measured results, which validates our idea.

References

[1] M. Yu and V. Miraftab, "Shrinking microwave filters," *IEEE Microw. Mag.*, vol. 9, no. 5, pp. 40–54, Oct. 2008.
[2] R. J. Cameron, C. M. Kudsia, and R. R. Mansour, *Microwave Filters for Communication Systems: Fundamentals, Design and Application*. Hoboken, NJ, USA: Wiley, 2007.
[3] M. Meng, I. C. Hunter, and J. D. Rhodes, "The design of parallel connected filter networks with nonuniform Q resonators," *IEEE Trans. Microw. Theory Techn.*, vol. 61, no. 1, pp. 372–381, Jan. 2013.
[4] V. Miraftab and M. Yu, "Advanced coupling matrix and admittance function synthesis techniques for dissipative microwave filters," *IEEE Trans. Microw. Theory Techn.*, vol. 57, no. 10, pp. 2429–2438, Oct. 2009.
[5] L.-F. Qiu, L.-S. Wu, W.-Y. Yin, and J.-F. Mao, "Lossy filter with uniform Q-factors by optimization method," in *Proc. Asia-Pacific Microw. Conf.*, Sendai, Japan, 2014, pp. 1300–1302.
[6] L. Szydlowski, A. Lamecki, and M. Mrozowski, "Design of microwave lossy filter based on substrate integrated waveguide (SIW)," *IEEE Microw. Wireless Compon. Lett.*, vol. 21, no. 5, pp. 249–251, May 2011.
[7] B. Gao, L.-S. Wu, and J.-F. Mao, "Lossy substrate integrated waveguide filter with flat passband," in *Proc. IEEE Int. Wireless Symp.*, Shanghai, China, Mar. 2016, pp. 1–4.